Int. J. Heat Mass Transfer. Vol. 15, pp. 2173–2186. Pergamon Press 1972. Printed in Great Britain

COUETTE FLOW WITH PARTICLE INJECTION

VICTOR QUAN*
TRW Systems, Redondo Beach, California 90278, U.S.A.

(*Received* 12 *March* 1971 *and in revised form* 13 *January* 1972)

Abstract—The steady flow of a viscous fluid between two infinite parallel flat walls with injection of particles from one wall and removal from the other is analyzed. The velocity and temperature distributions of the fluid and the particles are solved in analytical form for Stokes particle drag coefficient and in numerical form for constant coefficient. Arbitrary values of axial pressure gradient, viscous dissipation, particle injection angle and speed, and initial particle temperature are allowed. For the case of vertical injection and in the absence of axial pressure gradient, it is found that the wall shear stress is always decreased by particle injection whereas heat transfer can be increased or decreased. The dimensionless parameters which characterize the effects of particle injection on particle-free Couette flow are identified and discussed.

NOMENCLATURE

a, radius of a particle;
A, cross-sectional area of a particle;
A_s, surface area of a particle;
c_p, specific heat of fluid at constant pressure;
c_s, specific heat of particles;
C_D, particle drag coefficient;
F_{px}, horizontal force per unit volume exerted by particles on fluid;
F_{py}, vertical force per unit volume exerted by particles on fluid;
G, horizontal pressure gradient, $\partial p/\partial x$;
h, distance between walls;
H, particle heat-transfer coefficient;
I_i, modified Bessel function of first kind and order i;
k, fluid conductivity;
K_i, modified Bessel function of second kind and order i;
m, mass of a particle;
M, mass injection rate of particles, $\rho_{po}v_{po}$;
p, fluid pressure:
Pr, Prandtl number, $\mu c_p/k$;
q_0, heat flux to lower wall;
Q_p, heat transfer rate per unit volume from particles to fluid;
s, dimensionless constant, $2k/3\mu c_s$;
t, fluid temperature;
t_p, particle temperature;
T, dimensionless fluid temperature, $(t - t_0)/(t_\infty - t_0)$;
T_p, dimensionless particle temperature, $(t_p - t_0)/(t_\infty - t_0)$;
u, horizontal fluid velocity;
u_p, horizontal particle velocity;
U, dimensionless horizontal fluid velocity, u/u_∞;
U_p, dimensionless horizontal particle velocity, u_p/u_{p0};
v, vertical fluid velocity;
v_p, vertical particle velocity;
V_p, dimensionless vertical particle velocity, u_p/μ_{p0};
V_r, absolute relative velocity between fluid and particle;
w, dimensionless transformed variable, $(2aH/3k)^{\frac{1}{2}}z$;
x, distance in horizontal direction (parallel to wall);
y, distance in vertical direction (normal to wall);

*Present address: KVB Engineering Inc., 17332 Irvine Blvd., Tustin, California 92680.

Y, dimensionless vertical distance, y/h;
z, dimensionless transformed variable, $[4Mv_{p0}(1 - \beta hY/v_{p0})/\beta\mu]^{\frac{1}{2}}$;
β, constant, $6\pi a\mu/m$;
θ, dimensionless constant, $4\pi a^2Hh/mc_sv_{p0}$
λ, dimensionless variable, $\pi a^2\rho V_rC_Dh/2mv_{p0}$ (dimensionless constant, $6\pi a\mu h/mv_{p0}$ for Stokes flow);
μ, fluid viscosity;
ρ, mass of fluid per unit volume;
ρ_p, mass of particles per unit volume;
τ_0, shear stress at lower wall.

Subscripts

0, at lower wall which is stationary and where particles are injected;
∞, at upper wall which is moving and where particles are removed.

1. INTRODUCTION

THE SUBJECT of two-phase flow has received increasing attention in recent years due to its importance in modern engineering applications. Some classical papers on this subject have been written by Carrier on shock waves in a dusty gas [1], by Kliegel on gas-particle nozzle flow [2], and by Marble on fluid-particle boundary layer flow [3], among others. A description of many published papers on fluid dynamics of multiphase systems can be found in the book by Soo [4]. The majority of the problems treated, however, have been concerned with configurations where the particles are initially at equilibrium with or entrapped in the fluid. In such systems the particle streamlines are nearly parallel to the fluid streamlines, i.e. the particle moves *along* with the fluid. In the few studies that involve injection of particles into a fluid, only the particle trajectory is analyzed and the effects of particles on the fluid are usually neglected.

In the present study, particles are injected from a surface into a viscous fluid flowing between two parallel flat walls. The particle size, injection angle and speed, mass flux, and initial particle temperature are taken as arbitrary. The flow configuration is shown in Fig. 1. Solutions for the two-phase flow properties are obtained to show the mutual effects of interaction between the particles and the fluid.

One of the problems that led to the present study concerns the survivability of high-speed vehicles under erosive conditions. When a missile travels through a dust, rain, or ice environment, severe erosion of surface material may result due to particle bombardment. The eroded material leaves the surface in the form of small particles. The question then arises as to what effects will the eroded particles exert on the shear stress and heat flux at the missile surface. The answer to this question is important because the erosion rate is generally highly dependent on the surface shear stress and heat flux.

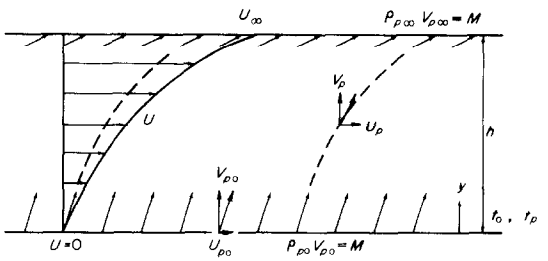

FIG. 1. Couette flow with particle injection.

Other important applications involving the injection of particles into boundary layers include soil saltation by natural winds, lunar surface erosion by a landing vehicle's exhaust, and dust entrainment by a nuclear explosion. In these problems, it is generally accepted that the amount of particles eroded from a surface due to aerodynamic forces is determined by the criterion that the amount of erosion is just sufficient to reduce the surface shear stress to a minimum restraining value. However, the accuracy of this prediction method has been severely limited because the effects of particle injection on the flowfield, and thus on the surface stress, have not been rigorously analyzed.

Although the Couette flow configuration does not precisely match an external boundary layer, it nevertheless illustrates the effects of particle injection on a viscous fluid flowfield and identifies many important parameters of the problem. Furthermore, Couette flow has the advantage of yielding a solution for the complete Navier–Stokes equations. In studies such as chemical non-equilibrium [5], magnetogas-dynamics [6], radiation absorption [7], etc., Couette flow has been considered as a standard of comparison for other more complicated flow configurations.

2. GOVERNING EQUATIONS

In the present analysis, the following important assumptions are made:

(1) The particles injected into the fluid are spherical in shape and uniform in size.

(2) Chemical reaction, mass transfer, and radiation between the particles and the fluid are not considered.

(3) Momentum transfer between particles and fluid is due only to drag and heat transfer due only to convection.

(4) The temperature is uniform within a particle.

(5) Interaction between particles themselves is not considered.

(6) Particles are injected from one wall at a given rate, and are removed from the other wall at the same rate.

(7) Continuum theory is applicable to the two-phase system.

The conservation equations for mass, x-momentum, y-momentum, and energy of the two-phase system can be written as

$$\frac{\partial}{\partial x}(\rho u + \rho_p u_p) + \frac{\partial}{\partial y}(\rho v + \rho_p v_p) = 0 \tag{1}$$

$$\rho\left(u\frac{\partial u}{\partial x} + v\frac{\partial u}{\partial y}\right) + \rho_p\left(u_p\frac{\partial u_p}{\partial x} + v_p\frac{\partial u_p}{\partial y}\right) + \frac{\partial_p}{\partial x} = \mu\left(\frac{\partial^2 u}{\partial x^2} + \frac{\partial^2 u}{\partial y^2}\right) \tag{2}$$

$$\rho\left(u\frac{\partial v}{\partial x} + v\frac{\partial v}{\partial y}\right) + \rho_p\left(u_p\frac{\partial v_p}{\partial x} + v_p\frac{\partial v_p}{\partial y}\right) + \frac{\partial p}{\partial y} = \mu\left(\frac{\partial^2 v}{\partial x^2} + \frac{\partial^2 v}{\partial y^2}\right) \tag{3}$$

$$\rho c_p\left(u\frac{\partial t}{\partial x} + v\frac{\partial t}{\partial y}\right) + \rho_p c_s\left(u_p\frac{\partial t_p}{\partial x} + v_p\frac{\partial t_p}{\partial y}\right) = k\left(\frac{\partial^2 t}{\partial x^2} + \frac{\partial^2 t}{\partial y^2}\right) + u\frac{\partial p}{\partial x} + v\frac{\partial p}{\partial y} + (u_p - u)F_{px} + (v_p - v)F_{py} + \mu\left[2\left(\frac{\partial u}{\partial x}\right)^2 + 2\left(\frac{\partial v}{\partial y}\right)^2 + \left(\frac{\partial v}{\partial x} + \frac{\partial u}{\partial y}\right)^2\right]. \tag{4}$$

Furthermore, for the particle phase, one may write

$$\frac{\partial}{\partial x}(\rho_p u_p) + \frac{\partial}{\partial y}(\rho_p v_p) = 0 \tag{5}$$

$$\rho_p\left(u_p\frac{\partial u_p}{\partial x} + v_p\frac{\partial u_p}{\partial y}\right) + F_{px} = 0 \tag{6}$$

$$\rho_p\left(u_p\frac{\partial v_p}{\partial x} + v_p\frac{\partial v_p}{\partial y}\right) + F_{py} = 0 \tag{7}$$

$$\rho_p c_s\left(u_p\frac{\partial t_p}{\partial x} + v_p\frac{\partial t_p}{\partial y}\right) + Q_p = 0. \tag{8}$$

The forces exerted on a unit volume of fluid by the particles can be written as

$$F_{px} = \tfrac{1}{2}(\rho_p/m)\,\rho A C_D V_r(u_p - u) \tag{9}$$

$$F_{py} = \tfrac{1}{2}(\rho_p/m)\,\rho A C_D V_r(v_p - v) \tag{10}$$

where

$$V_r = [(u_p - u)^2 + (v_p - v)^2]^{\frac{1}{2}}. \tag{11}$$

The heat transfer from the particles to a unit volume of fluid can be written as

$$Q_p = (\rho_p/m)\,H A_s(t_p - t). \tag{12}$$

The boundary conditions are

$$\begin{aligned} &v = 0, u = 0, t = t_0 && \text{at } y = 0\\ &u = u_\infty, t = t_\infty && \text{at } y = h\\ &\rho_p = \rho_{p0}, u_p = u_{p0}, v_p = v_{p0}, t_p = t_{p0} && \text{at } y = 0 \end{aligned} \tag{13}$$

where t_0, u_∞, t_∞, ρ_{p0}, v_{p0} and t_{p0} are constants. In addition, Couette flow herein is considered to be one in which the gradients of ρ, u, t, ρ_p, u_p and T_p are zero in the x-direction. Equations (1)–(13) then completely define the mathematical model, assuming expressions for ρ and C_D are given. The solution is presented in the following section.

3. SOLUTION

For Couette flow, equations (1) and (5) and the condition of $v = 0$ at $y = 0$ yield

$$v = 0 \tag{14}$$

$$\rho = \rho(y) \tag{15}$$

$$\rho_p v_p = \rho_{p0} v_{p0} = M \tag{16}$$

where M is the constant mass flux of particle injection. Equations (2)–(4) become

$$M\frac{\mathrm{d}u_p}{\mathrm{d}y} + \frac{\partial p}{\partial x} = \mu\frac{\mathrm{d}^2 u}{\mathrm{d}y^2} \tag{17}$$

$$M\frac{\mathrm{d}v_p}{\mathrm{d}y} + \frac{\partial p}{\partial y} = 0 \tag{18}$$

$$Mc_s\frac{\mathrm{d}t_p}{\mathrm{d}y} = k\frac{\mathrm{d}^2 t}{\mathrm{d}y^2} + u\frac{\partial p}{\partial x} - M(u_p - u)\frac{\mathrm{d}u_p}{\mathrm{d}y} - Mv_p\frac{\mathrm{d}v_p}{\mathrm{d}y} + \mu\left(\frac{\mathrm{d}u}{\mathrm{d}y}\right)^2 \tag{19}$$

and equations (6)–(8) become

$$v_p\frac{\mathrm{d}u_p}{\mathrm{d}y} + \frac{1}{2}\frac{\rho}{m}AC_D V_r(u_p - u) = 0 \tag{20}$$

$$v_p\frac{\mathrm{d}v_p}{\mathrm{d}y} + \frac{1}{2}\frac{\rho}{m}AC_D V_r v_p = 0 \tag{21}$$

$$v_p\frac{\mathrm{d}t_p}{\mathrm{d}y} + \frac{HA_s}{mc_s}(t_p - t) = 0. \tag{22}$$

Equation (18) yields the solution for p in the form

$$p(x, y) = p(x, 0) - M(v_p - v_{p0}) \tag{23}$$

and equation (17) requires $\partial p/\partial x$ to be a function of y only. Using equation (23), one obtains

$$\frac{\partial p}{\partial x} = \frac{\mathrm{d}p(x, 0)}{\mathrm{d}x} = \text{constant} \equiv G \tag{24}$$

where a positive value of G corresponds to an increase in pressure as the fluid flows downstream.

Equations (17) and (19) can be integrated once and reduced to

$$\mu\frac{\mathrm{d}u}{\mathrm{d}y} - Gy - Mu_p = C_1 = \tau_0 - Mu_{p0} \tag{25}$$

$$k\frac{\mathrm{d}t}{\mathrm{d}y} - Mc_s t_p + Guy + (\tau_0 - Mu_{p0})u + Muu_p - \frac{M}{2}(u_p^2 + v_p^2) = C_2 = q_0 - Mc_s t_{p0} - \frac{M}{2}(u_{p0}^2 + v_{p0}^2) \tag{26}$$

where C_1 and C_2 are constants of integration and can be replaced by quantities expressed in terms of τ_0 and q_0.

It is observed at this point that three of the eight governing differential equations may be eliminated since they have been used to solve for v, p and ρ_p where $\rho_p = M/v_p$. It may also be noted that $\rho(y)$ can be left as arbitrary since an equation of state has not been specified; however, the conditions of $\partial\rho/\partial x = \partial t/\partial x = 0$ imply $\partial p/\partial x = 0$ except for incompressible flow for which ρ is a constant and not related to p and t. In Couette flow, density has no effect on the velocity and temperature distributions. The reason is that the convective terms in the momentum and energy equations vanish identically as seen in equations (25) and (26). It is true that to solve for $\rho(y)$, one must prescribe an equation of state. However, $\rho(y)$ is not of importance in the present analysis since the drag force and heat transfer between particle and fluid are independent of fluid density for both Stokes flow and constant-ρC_D flow.

It is advantageous to non-dimensionalize the five remaining differential equations which govern u, t, u_p, v_p and t_p. Let

$$Y = \frac{y}{h}, U = \frac{u}{u_\infty}, T = \frac{t - t_0}{t_\infty - t_0}$$

$$U_p = \frac{u_p - u_{p0}}{u_\infty}, V_p = \frac{v_p}{v_{p0}}, T_p = \frac{t_p - t_{p0}}{t_\infty - t_0}. \quad (27)$$

Equations (25), (26) and (20)–(22) can then be written as

$$\frac{dU}{dY} - \frac{Gh^2}{\mu u_\infty} Y - \frac{Mh}{\mu} U_p = \frac{h\tau_0}{\mu u_\infty} \quad (28)$$

$$\frac{dT}{dY} - \frac{Mc_s h}{k} T_p = \frac{h}{k(t_\infty - t_0)} \left[q_0 - \frac{\mu u_\infty^2}{h} U \frac{dU}{dY} + \frac{M}{2} (v_{p0}^2 V_p^2 - v_{p0}^2 + u_\infty^2 U_p^2 + 2u_\infty u_{p0} U_p) \right] \quad (29)$$

$$V_p \frac{dU_p}{dY} + \frac{\rho A C_D V_r h}{2mv_{p0}} \left(\frac{u_{p0}}{u_\infty} + U_p - U \right) = 0 \quad (30)$$

$$\frac{dV_p}{dY} + \frac{\rho A C_D V_r h}{2mv_{p0}} = 0 \quad (31)$$

$$V_p \frac{dT_p}{dY} + \frac{A_s H h}{mc_s v_{p0}} \left(\frac{t_{p0} - t_0}{t_\infty - t_0} + T_p - T \right) = 0. \quad (32)$$

The variables U, T, U_p, V_p and T_p and the unknown constants τ_0 and q_0 are subject to the boundary conditions of

$$\begin{aligned} &U = T = U_p = T_p = 0 && \text{at } y = 0 \\ &V_p = 1 && \text{at } Y = 0 \\ &U = T = 1 && \text{at } Y = 1. \end{aligned} \quad (33)$$

For values of C_D that are nonlinear functions of V_r, equations (28)–(33), which are nonlinear and involve two-point boundary conditions, must be solved numerically in general. Some numerical results, which are obtained by using the standard Runge–Kutta–Adams–Moulton numerical integration procedure, for constant ρ and C_D are shown in a latter section. For Stokes flow regime (low particle Reynolds numbers), however, C_D is inversely proportional to ρV_r and the solution can be obtained analytically as shown below.

For Stokes flow ($C_D = 12\mu/a\rho V_r$), equation (31) and the boundary condition of $V_p = 1$ at $Y = 0$ yield

$$V_p = 1 - \beta h Y / v_{p0} \quad (34)$$

where

$$\beta = 6\pi a\mu/m. \quad (35)$$

Here, it should be noted that in order for ρ_p to be bounded, v_p must be positive everywhere since $\rho_p = M/v_p$. This implies $\beta h < v_{p0}$ according to equation (34). That is, the vertical injection velocity must be sufficiently high to overcome drag so that the particles can reach and be removed at the upper wall; otherwise, there is accumulation of mass in the flow and the Couette flow condition does not exist.

With V_p being known, equations (28) and (30) can be used to solve for U_p and U simultaneously. The result is

$$U_p = z[C_3 I_1(z) + C_4 K_1(z)] - \frac{1}{Mu_\infty} \times \left(\tau_0 + \frac{Gv_{p0}}{\beta} - \frac{G\mu}{4M} z^2 \right) \quad (36)$$

$$U = \tfrac{1}{2} z^2 [-C_3 I_2(z) + C_4 K_2(z)] - \frac{1}{Mu_\infty} \times \left(\tau_0 + \frac{Gv_{p0}}{\beta} - Mu_{p0} \right) \quad (37)$$

where z is a function of Y:

$$z = \left[4Mv_{p0} \left(1 - \frac{\beta h}{v_{p0}} Y \right) \Big/ \beta\mu \right]^{\frac{1}{2}} \quad (38)$$

and where I_i and K_i are the modified Bessel functions of first and second kind, respectively, and of order i. The constants C_3, C_4 and τ_0 are determined by the conditions of $U_p = U = 0$ at $Y = 0$ and $U = 1$ at $Y = 1$, and have the values of

$$C_3 = \frac{-K_0(z_0) + \frac{1}{Mu_\infty}\left(Mu_{po} - \frac{Gv_{po}}{\beta}\right)\left[K_2(z_0) - \left(\frac{z_h}{z_0}\right)^2 K_2(z_h)\right]}{1 + \frac{z_h^2}{2}\left[K_0(z_0)I_2(z_h) - I_0(z_0)K_2(z_h)\right]} \tag{39}$$

$$C_4 = \frac{1}{K_0(z_0)}\left[C_3 I_0(z_0) - \frac{2}{z_0^2}\left(\frac{u_{p0}}{u_\infty} - \frac{Gv_{po}}{\beta M u_\infty}\right)\right] \tag{40}$$

$$\tau_0 = Mu_\infty z_0[C_3 I_1(z_0) + C_4 K_1(z_0)] \tag{41}$$

where z_0 and z_h denote z evaluated at $Y = 0$ and $Y = 1$, respectively.

With V_p, U_p and U being known, equations (29) and (32) can be used to determine T_p and T simultaneously. The result is

$$T_p = w^s I_s(w)\left[C_5 + A(w)\right] + w^s I_{-s}(w) \times \left[C_6 - B(w)\right] - \frac{q_0}{Mc_s(t_\infty - t_0)} \tag{42}$$

$$T = \frac{1}{2s} w^{s+1}\left\{I_{s+1}(w)\left[C_5 + A(w)\right] + I_{-s-1}(w) \times \left[C_6 - B(w)\right]\right\} - \frac{q_0}{Mc_s(t_\infty - t_0)} + \frac{t_{p0} - t_0}{t_\infty - t_0} \tag{43}$$

where w is related to Y through z:

$$w = (2aH/3k)^{\frac{1}{2}} z \tag{44}$$

and s is given by

$$s = 2k/3\mu c_s = 2c_p/3Prc_s. \tag{45}$$

In equations (42) and (43), the functions $A(w)$ and $B(w)$ are given by

$$A(w) = \frac{\pi}{2\sin(s\pi)} \int_{w_0}^{w} \bar{w}^{1-s} I_{-s}(\bar{w})\,\psi(\bar{w})\,d\bar{w} \tag{46}$$

$$B(w) = \frac{\pi}{2\sin(s\pi)} \int_{w_0}^{w} \bar{w}^{1-s} I_{s}(\bar{w})\,\psi(\bar{w})\,d\bar{w} \tag{47}$$

where

$$\psi(w) = \frac{u_\infty^2}{2c_s(t_\infty - t_0)}\left[2\left(\frac{u_{p0}}{u_\infty}\right)U_p + U_p^2 + \left(\frac{v_{p0}}{u_\infty}\right)^2 \times (V_p^2 - 1) - \frac{2U}{M}\left(\frac{\tau_0}{u_\infty} + \frac{Gh}{u_\infty} Y + MU_p\right)\right]. \tag{48}$$

The constants C_5, C_6 and q_0 are determined by the conditions of $T_p = T = 0$ at $Y = 0$ and $T = 1$ at $Y = 1$, and have the values of

$$C_5 = (C_{5a} - C_{5b})/C_{5c}$$

$$C_{5a} = I_{-s+1}(w_0)\left\{1 + \frac{1}{2s} w_h^{s+1}\left[I_{s+1}(w_h)A(w_h) - I_{-s-1}(w_h)B(w_h)\right]\right\} \tag{49}$$

$$C_{5b} = \left(\frac{t_{po} - t_0}{t_\infty - t_0}\right) \times \left[I_{-s-1}(w_0) - \left(\frac{w_h}{w_0}\right)^{s+1} I_{-s-1}(w_h)\right]$$

$$C_{5c} = \frac{2}{\pi} w_0^{s-1} \sin(s\pi) + \frac{1}{2s} w_h^{s+1} \left[I_{s-1}(w_0)I_{-s-1}(w_h) - I_{-s+1}(w_0)I_{s+1}(w_h)\right]$$

$$C_6 = \frac{1}{I_{-s+1}(w_0)} \left[-C_5 I_{s-1}(w_0) + 2s w_0^{-s-1} \left(\frac{t_{po} - t_0}{t_\infty - t_0}\right)\right] \tag{50}$$

$$q_0 = Mc_s(t_\infty - t_0) w_0^s [C_5 I_s(w_0) + C_6 I_{-s}(w_0)] \tag{51}$$

where w_0 and w_h denote w evaluated at $Y = 0$ and $Y = 1$, respectively.

Equations (42)–(51) are applicable to non-integral values of s. If s is equal to an integer n, the following modifications are to be made: In equations (42) and (43), I_{-s} and I_{-s-1} are replaced by K_n and $-K_{n+1}$, respectively. In equations (46) and (47), the coefficient $\pi/2 \sin s\pi$ is deleted. The function I_{-s} in equations (46) and (51) is replaced by K_n, and I_{-s+1} in equation (50) is replaced by $-K_{n-1}$. Finally, in equation (49), I_{-s+1} is replaced by $-K_{n-1}$, I_{-s-1} is replaced by $-K_{n+1}$, and the coefficient $(2/\pi) \sin s\pi$ is deleted.

Although the convective heat-transfer coefficient, H, has been left as an arbitrary constant, it may be noted that the Nusselt number, $Nu = Ha/k$, is unity for Stokes flow. For $Ha/k = 1$, equation (44) can be replaced by $w = (2/3)^{\frac{1}{2}}z$. It may also be noted that for many common gases, the Prandtl number, $Pr = \mu c_p/k$, is approximately equal to 2/3. The value of s given by equation (45) then becomes $s = c_p/c_s$. If, furthermore, the gas and the particles have similar specific heats, then s is on the order of unity.

4. RESULTS

Equations (28) to (32) show that V_p, U, U_p, T and T_p have the following functional form:

$$V_p = V_p(Y, \lambda)$$

$$U, U_p = U, U_p\left(Y, \lambda, \frac{Gh^2}{\mu u_\infty}, \frac{Mh}{\mu}, \frac{u_{p0}}{u_\infty}\right) \tag{52}$$

$$T, T_p = T, T_p\left(Y, \lambda, \frac{Gh^2}{\mu u_\infty}, \frac{Mh}{\mu}, \frac{u_{p0}}{u_\infty}, \theta, \frac{Mhc_s}{k} \text{ or } \frac{c_s\mu}{k}, \frac{\mu u_\infty^2}{k(t_\infty - t_0)}, \frac{t_{p0} - t_0}{t_\infty - t_0}, \frac{v_{p0}}{u_\infty}\right)$$

where

$$\lambda = \pi a^2 \rho V_r C_D h/2mv_{p0}$$
$$\theta = 4\pi a^2 Hh/mc_s v_{p0}. \tag{53}$$

The dimensionless groups may be interpreted as the ratios of various effects:

Y = distance from injection surface/distance between walls
λ = drag on a particle/inertia of a particle
$Gh^2/\mu u_\infty$ = pressure force/viscous force
Mh/μ = force exerted by particles/viscous force
θ = heat convection to a particle/heat absorption by a particle
$c_s\mu/k$ = absorption of viscous energy by particle/heat conduction by fluid
$\mu u_\infty^2/k(t_\infty - t_0)$ = viscous energy dissipation/heat conduction by fluid
u_{p0}/u_∞ = initial axial particle velocity/fluid velocity
v_{p0}/u_∞ = initial vertical particle velocity/fluid velocity
$(t_{p0} - t_0)/(t_\infty - t_0)$ = initial relative particle temperature/fluid temperature (54)

The ten dimensionless groups cover eighteen physical variables: y, h, μ, k, H, ρ, C_D, $\partial p/\partial x$, a, m, c_s, u_∞, t_0, t_∞, u_{p0}, v_{p0}, t_{p0}, and ρ_{p0}. Equation (52) shows T and T_p to depend on all ten groups. If λ is a constant (Stokes flow), then V_p depends only on two groups and U and U_p on five groups. However, for general ρ and C_D, the values of V_p, U and U_p also depend on all ten groups since λ varies with T, U and U_p through the dependencies of ρ on T and V_r on U and U_p. The results for the cases of constant ρ (for these cases, V_p, U_p and U become independent of the T and T_p, but not vice versa) and constant C_D (for cases involving high Reynolds numbers) are illustrated later in this section. Here, the primary interest is on Stokes flow for which

$$\lambda = \beta h/v_{p0} = 6\pi a\mu h/mv_{p0}. \tag{55}$$

The results for Stokes flow are presented in Figs. 2–11. Since the solution depends on many dimensionless parameters, only selected results will be chosen here for illustration. Readers interested in other results may employ

the analytical solution given by equations (34)–(51). In the figures, U and V refer to u and v, respectively, in the text.

The values of V_p, which can be seen from equation (34) to depend only on and to vary linearly with λY, are shown in Fig. 2. The variations of U and U_p which depend on five parameters are shown in Figs. 3–6. Figure 3 shows the variations of u/u_∞ and u_p/u_∞ with y/h for

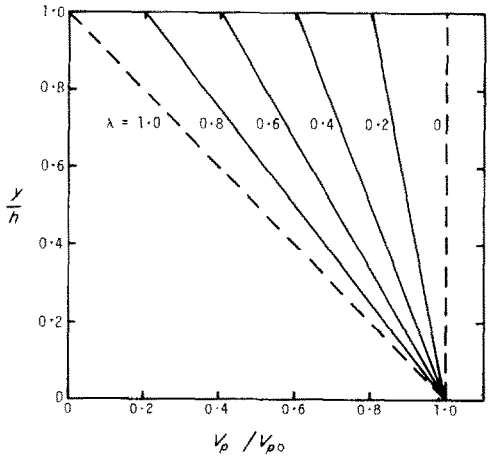

FIG. 2. v_p/v_{p0} as a function of λ and y/h.

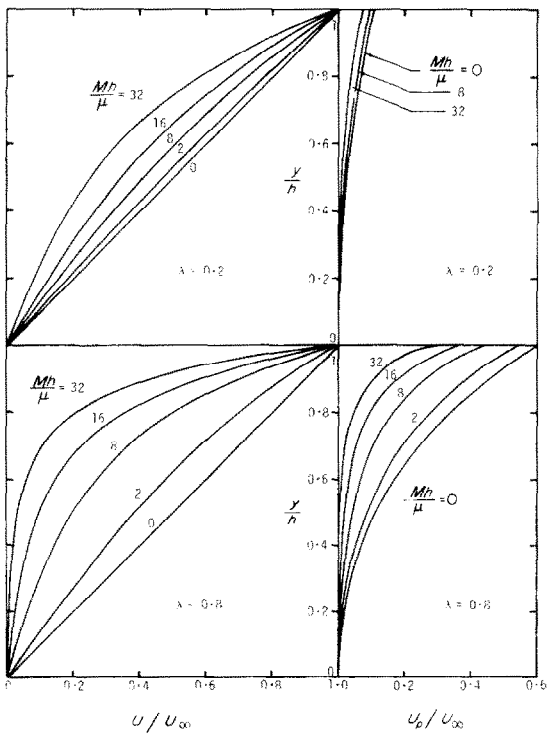

FIG. 3. Fluid and particle velocity distributions ($u_{p0} = G = 0$).

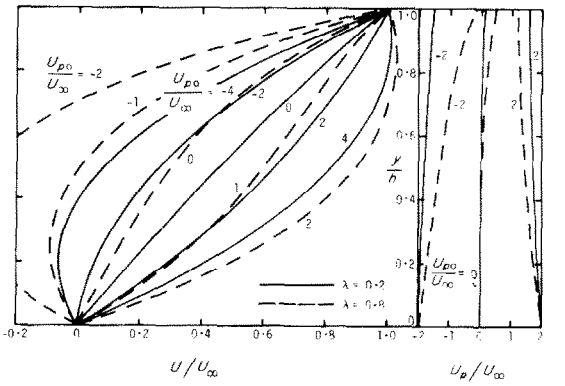

FIG. 4. Effects of u_{p0}/u_∞ on u/u_∞ and u_p/u_∞ ($G = 0$ and $Mh/\mu = 4$).

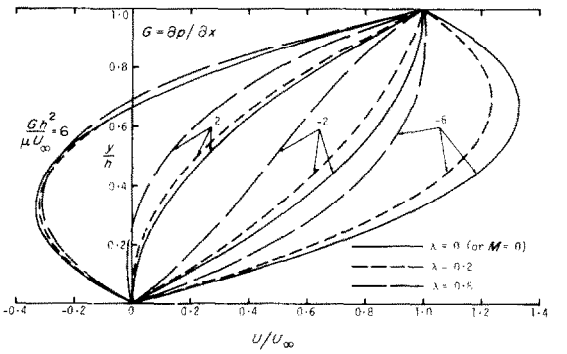

FIG. 5. Effects of particle injection on flows with finite axial pressure gradients ($u_{p0} = 0$ and $Mh/\mu = 4$).

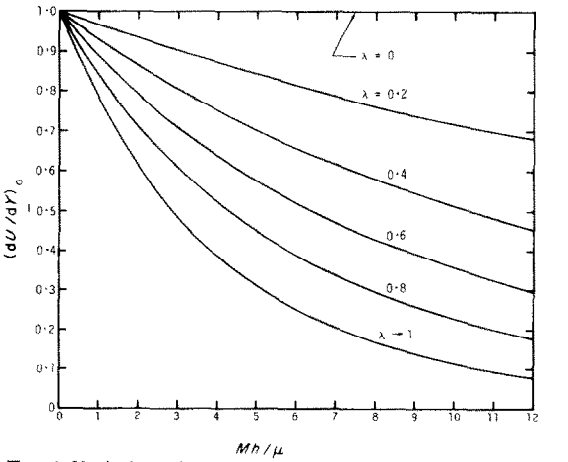

FIG. 6. Variation of normalized wall shear stress with Mh/μ and λ ($u_{p0} = G = 0$).

several values of Mh/μ and λ; the results here correspond to the case of vertical injection ($u_{p0}/u_\infty = 0$) and zero axial pressure gradient ($Gh^2/\mu u_\infty = 0$). From Fig. 3, it is seen that particle injection lowers the shear stress (or fluid velocity gradient) at the injection surface and that the distortion of the flowfield becomes more extensive as the mass flux of injection, M, increases. It is also seen that the effects of particle injection are greater for larger values of λ; the reason for this is that larger λ corresponds to longer stay time of particle in fluid which results in greater particle–fluid relaxation effects.

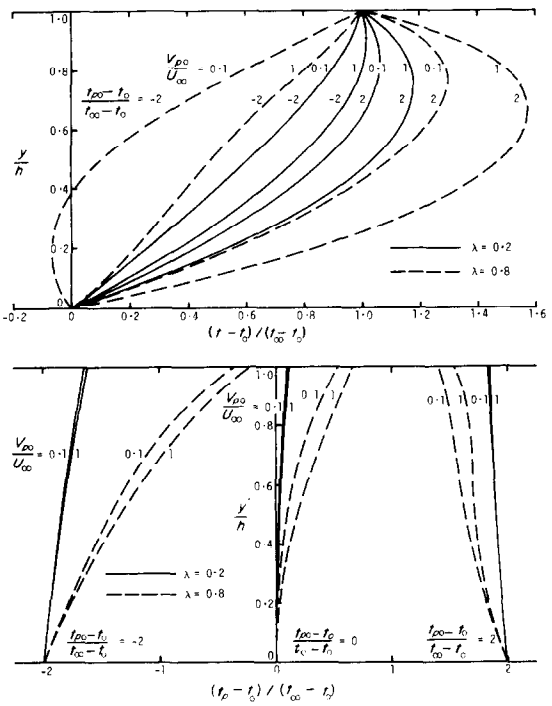

FIG. 7. Fluid and particle temperature distributions [$u_{p0} = G = 0$, $c_s\mu/k = 1$, $\mu u_\infty^2/k(t - t_0) = 2$, and $Mh/\mu = 4$].

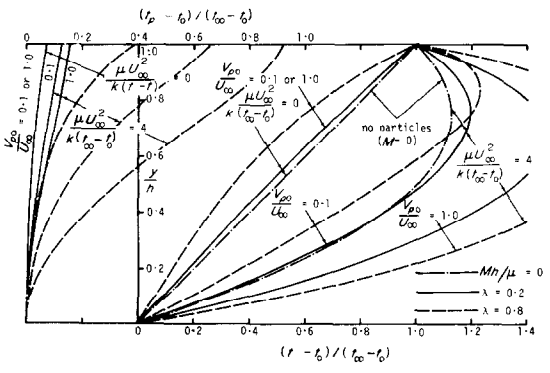

FIG. 8. Effects of $\mu u_\infty^2/k(t_\infty - t_0)$ and v_{p0}/u_∞ on $(t - t_0)/(t_\infty - t_0)$ and $(t_p - t_0)/(t_\infty - t_0)$, ($u_{p0} = G = t_{p0} - t_0 = 0$, $c_s\mu/k = 1$, and $Mh/\mu = 4$).

For vertical injection, the particles lower the surface shear stress because they absorb momentum from the fluid. However, if they are injected at finite angles from the normal (i.e. $u_{p0}/u_\infty \neq 0$), the shear stress or velocity profiles are altered in a different manner. The effects of the horizontal component of the injection velocity are illustrated in Fig. 4 in which it can be seen that significantly positive values of u_{p0}/u_∞ tend to increase the shear stress while near zero or negative values will decrease it. The particle velocity can be seen from Figs. 3 and 4 to approach the upper wall velocity (i.e. $u_p/u_\infty \to 1$) regardless of its initial value. In Fig. 5, the changes in velocity profile due to injection of particles into flows of finite axial pressure gradients are illustrated for the conditions of vertical injection and $Mh/\mu = 4$. Finally, the nondimensionalized shear stress at the lower wall, $(dU/dY)_0$, is shown as a function of λ and Mh/μ in Fig. 6 for vertical injection and zero axial pressure gradient. It is seen that drastic reductions of the wall shear stress due to particle injection are possible.

The results of T and T_p depend on ten parameters. One parameter, say θ, can be eliminated by considering Stokes flow for particle heat transfer (i.e. $Ha/k = 1$) which implies $\theta = (2\lambda/3)(k/\mu c_s)$. Figure 7 shows the effects of the injection velocity and initial particle-fluid temperature difference on the fluid and particle temperature profiles for the conditions of $u_{p0} = G = 0$, $\mu u_\infty^2/k(t_\infty - t_0) = 2$, $Mh/\mu = 4$, and $c_s\mu/k = 1$. It is seen that higher injection velocity results in higher fluid temperature and wall heat transfer, that positive and negative values of $(t_{p0} - t_0)$ correspond to higher and lower fluid temperatures, respectively, that the particles relax towards the upper wall tempera-

ture as they penetrate the fluid [i.e. $(t_p - t_0)/(t_\infty - t_0) \to 1$], and that larger λ results in greater influence of particles on fluid.

Figure 8 illustrates the fluid and particle temperature distributions for $\mu u_\infty^2/k(t_\infty - t_0) = 0$ and 4. It is seen that for $\mu u_\infty^2/k(t_\infty - t_0) = 0$, the effect of particle injection is to decrease the fluid temperature and the results are identical for $v_{p0}/u_\infty = 0{\cdot}1$ and 1. The reason for this is that as $\mu u_\infty^2/k(t_\infty - t_0) \to 0$, the viscous dissipation of the particle kinetic energy is negligible compared to the fluid thermal energy even for high values of v_{p0}/u_∞; and the fluid temperature is lowered by the absorption of thermal energy by the particles. On the other hand, for $\mu u_\infty^2/k(t_\infty - t_0) = 4$, particle injection can either increase or decrease the wall heat transfer. It is interesting to observe that low v_{p0}/u_∞ allows the particles to absorb energy from the fluid near the injection surface and thus to lower the wall heat transfer; whereas for high v_{p0}/u_∞, the transformation of the particle kinetic energy into heat outweighs the absorption of fluid thermal energy and results in higher wall heat transfer. One thus may generalize that particle injection lowers the wall shear stress due to absorption of momentum from the fluid; but it may increase or decrease the wall heat transfer, depending primarily on the relative effects of particle kinetic energy dissipation and thermal energy absorption.

The effects of $c_s\mu/k$ are illustrated in Fig. 9 and are seen to be more significant on the temperature distribution of the particles than of the fluid. Figure 10 shows the nondimensionalized heat-transfer rate at the lower wall, $(\mathrm{d}T/\mathrm{d}Y)_0$, as a function of v_{p0}/u_∞ for several values of $(t_{p0} - t_0)/(t_\infty - t_0)$ and λ and for $u_{p0} = G = 0$, $c_s\mu/k = 1$, $Mh/\mu = 4$ and $\mu u_\infty^2/k(t_\infty - t_0) = 2$. Figure 11 shows that $(\mathrm{d}T/\mathrm{d}Y)_0$ varies almost linearly with Mh/μ and that small and large values of v_{p0}/u_∞, respectively, tend to decrease and increase the heat transfer rate.

The results of Figs. 2–11 correspond to Stokes flow for which λ and θ as given by equation (53) are constants. At high particle Reynolds numbers, Stokes flow is not applicable and λ and θ become dependent on the flow properties. For non-Stokes flow, equations (28)–(33) must be solved numerically in generally. Consider the case of constant ρ, C_D and H. Then θ remains constant while λ becomes

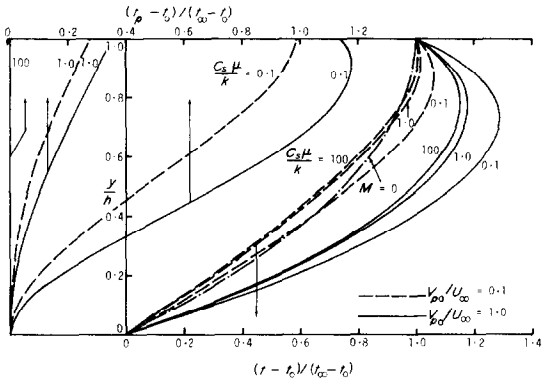

FIG. 9. Effects of $c_s\mu/k$ and v_{p0}/u_∞ on $(t - t_0)/(t_\infty - t_0)$ and $(t_p - t_0)/(t_\infty - t_0)$, $[u_{p0} = G = t_{p0} - t_0 = 0$, $\lambda = 0{\cdot}5$, $\mu u_\infty^2/k(t_\infty - t_0) = 2$, and $Mh/\mu = 4]$.

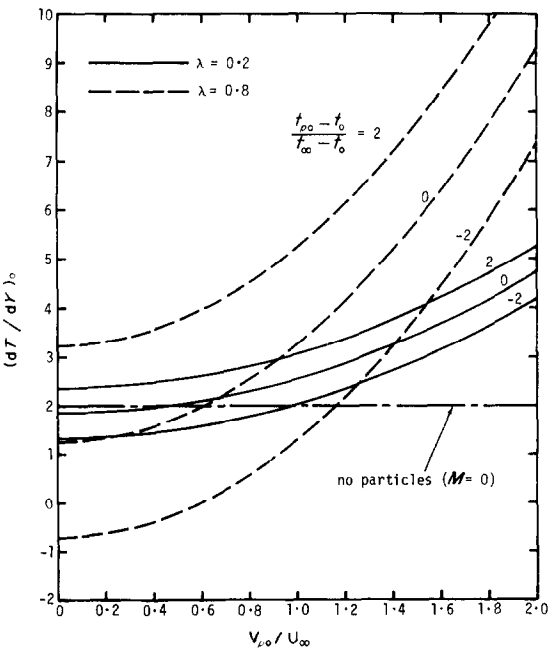

FIG. 10. Variation of normalized wall heat transfer with v_{p0}/u_∞, λ and $(t_{p0} - t_0)/(t_\infty - t_0)$, $[u_{p0} = G = 0$, $c_s\mu/k = 1$, $\mu u_\infty^2/k(t_\infty - t_0) = 2$, and $Mh/\mu = 4]$.

$$\lambda = \lambda_0 V_r / V_{r0} \tag{56}$$

where V_{r0} is V_r at $Y = 0$ and λ_0 is given by

$$\lambda_0 = \pi a^2 \rho V_{r0} C_D h / 2 m v_{p0}. \tag{57}$$

Some numerical results for constant ρ, C_D and H are shown in Fig. 12. The results of Stokes flow for which $\lambda = 6\pi a\mu h/mv_{p0}$ and $\theta = (2\lambda/3)(k/\mu c_s)$ are also shown for comparison. In Fig. 12, the variations of V_p, U, U_p, T and T_p with Y are shown for three sample combinations of λ_0 and v_{p0}/u_∞. The results of V_p, U and U_p are independent of θ. It is seen that the effects of particle injection on U are greater with constant ρC_D flow than with Stokes flow for small values of λ_0 and v_{p0}/u_∞, and vice versa for large values of λ_0 and v_{p0}/u_∞; and that for some combinations of λ_0 and v_{p0}/u_∞, constant ρC_D flow yields nearly identical results as Stokes flow. The effects of θ on T and T_p are also illustrated in Fig. 12. Larger values of θ correspond to higher heat transfer between particles and fluid and are seen to result in lower temperature difference between the two phases.

In addition to the results given above for V_p, U, U_p, T and T_p, it may be noted that ρ_p is equal to M/v_p, v is zero, ρ is arbitrary and can be determined by an equation of state such as $\rho = \rho(p, T)$ or $\rho =$ constant, and p is given by equation (23). It may also be pointed out that two fluid properties, ρ and c_p, are unimportant in this problem (except for the influence of ρ on particle drag for non-Stokes flow); because in the conservation equations, the transport terms involving inertia and heat convection within the fluid vanish for Couette flow. The conductivity of the particles is also unimportant because it has been assumed that the conductivity is sufficiently high and the particle size is sufficiently small for the temperature to be uniform within a particle.

Because of the large number of parameters, which are inherent in two-phase flow systems, and of their wide range in values, all of the results illustrated in this paper appear physically achievable. The figures showing the effects of

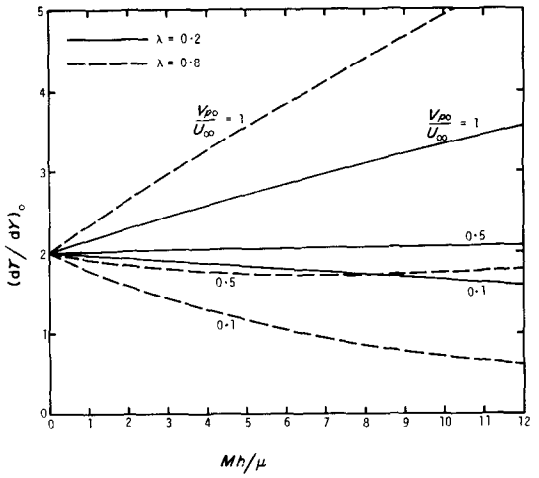

FIG. 11. Variation of normalized wall heat transfer with Mh/μ, v_{p0}/u_∞, and λ, [$u_{p0} = G = t_{p0} - t_0 = 0$, $c_s\mu/k = 1$, and $\mu u_\infty^2/k(t_\infty - t_0) = 2$].

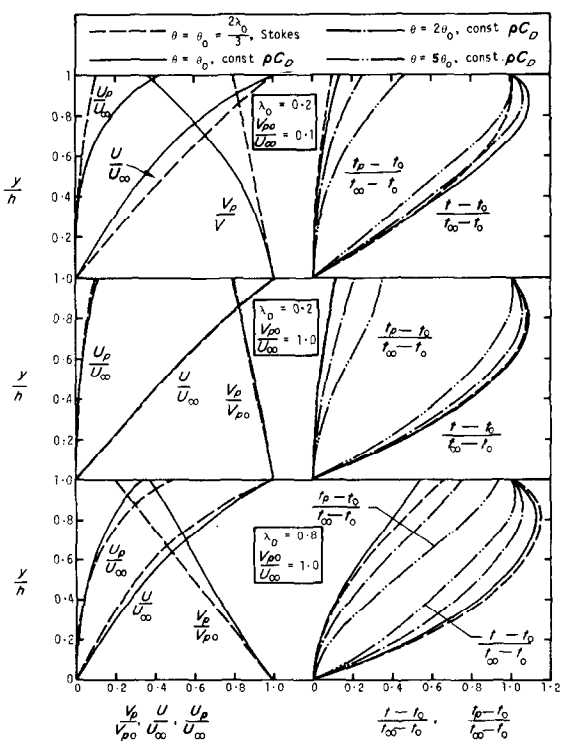

FIG. 12. Constant ρC_D flow compared to Stokes flow [$u_{p0} = G = t_{p0} - t_0 = 0$, $c_s\mu/k = 1$, $\mu u_\infty^2/k(t_\infty - t_0) = 2$, and $Mh/\mu = 4$].

pressure gradient and viscous energy dissipation resemble those shown in textbooks for particle-free Couette flow. The ratios of particle to fluid initial velocities and temperatures as illustrated can be reasonably expected. It is of significant interest, however, to demonstrate, by way of a sample missile erosion problem, the range of effects of particle injection using the Couette flow results. To simulate this problem, one may approximate the boundary layer thickness by h, free stream velocity by u_∞, and stagnation or reference temperature by t_∞. Consider the material being eroded from the missile surface to have a mass density ρ_m of 900 kg/m^3 (the mass of a particle m is equal to $4\pi a^3\rho_m/3$), specific heat c_s of 10^3 m^2/s$^2-{}^\circ$K, and average radius a of 5 microns. Also, take $h = 0{\cdot}01$ m, $\mu = 10^{-4}$ kg/m-s, $k = 0{\cdot}1$ kg-m/s$^3-{}^\circ$K, $\rho = 0{\cdot}01$ kg/m^3, $G = 0$, $u_\infty = v_{p0} = 10^3$ m/s, $u_{p0} = 0$, $t_\infty - t_0 = 500^\circ$K, $t_{p0} - t_0 = 0$ and $M = 0{\cdot}1$ kg/m^2-s. The particle Reynolds number here can be shown to be sufficiently small for Stokes flow to be applicable. For the above values one obtains $c_s\mu/k = 1$, $\mu u_\infty^2/k(t_\infty - t_0) = 2$, $v_{p0}/u_\infty = 1$, $\lambda = 0{\cdot}2$ and $Mh/\mu = 10$. Then from Fig. 6, one observes that the surface stress is reduced by nearly 30 per cent from the particle-free value; and from Fig. 11, one observes the heat flux to be increased by a factor of about 1·6. However, if the particle radius a is 2·5 instead of 5 microns and the mass erosion rate M is 0·01 instead of 0·1 kg/m^2 s, then $\lambda = 0{\cdot}8$ and $Mh/\mu = 1$; and the shear stress and heat flux will differ accordingly. This illustrates the wide range of parameters that may be encountered. For turbulent boundary layers, h may be taken as the thickness of the laminar sublayer. Under severe erosive conditions, M may be orders of magnitude greater than the numbers illustrated.

5. SUMMARY AND CONCLUSIONS

From the present analysis, one may summarize and conclude that:

(1) A solution for Couette flow with injection of particles has been obtained in analytical form for Stokes particle drag coefficient and in numerical form for constant drag coefficient. The velocity and temperature distributions of the fluid and the particles are found to depend on ten dimensionless groups which cover eighteen physical variables.

(2) The injected particles can penetrate the channel depth only if $6\pi a\mu h/mv_{p0} < 1$ for Stokes flow. For flows with constant ρC_D, this condition is approximately equivalent to $\pi a^2\rho C_D V_{r0}h/2mv_{p0} < 1$.

(3) Larger value of λ_0, where $\lambda_0 = 6\pi a\mu h/mv_{p0}$ for Stokes flow and $\lambda_0 = \pi a^2\rho C_D V_{r0}h/2mv_{p0}$ for constant ρC_D flow, yields greater particles–fluid relaxation effects.

(4) The effects of particle injection on a fluid flowfield increase with Mh/μ.

(5) Particle injection generates a pressure gradient in the direction normal to the walls due to conversion of vertical particle momentum to hydrodynamic pressure.

(6) For normal injection and zero horizontal pressure gradient, particle injection is found to always decrease the velocity gradient or shear stress at the injection surface. This is due to transfer of horizontal momentum from fluid to particles.

(7) Normal injection tends to neutralize the effects of the horizontal pressure gradient on the fluid velocity distribution, especially if the gradient is negative (i.e. decreasing pressure in direction of flow).

(8) The injection angle affects the flow in such a manner that large positive values of u_{p0}/u_∞ tend to increase the wall shear stress while near zero or negative values will decrease it.

(9) When viscous dissipation effects are small, i.e. $\mu u_\infty^2/k(t_\infty - t_0) \to 0$, particle injection is found to decrease the temperature gradient or heat transfer at the injection surface (unless the particle initial temperature is higher than the wall temperature). This is due to heat transfer from fluid to particles.

(10) When viscous dissipation effects are significant, i.e. $\mu u_\infty^2/k(t_\infty - t_0) = 0(1)$, particle injection is found to increase or decrease the

heat transfer at the injection surface for large or small values of v_{p0}/u_∞, respectively. For large v_{p0}/u_∞, substantial amount of particle kinetic energy is introduced into the flow; if $\mu u_\infty^2/k(t_\infty - t_0)$ is not small, the conversion of particle kinetic energy into viscous heat dissipation outweighs the particle absorption of fluid thermal energy and results in the increase of wall heat transfer. However, for small v_{p0}/u_∞, the particle kinetic energy is negligible and the particle absorption of fluid thermal energy results in a decrease of wall heat transfer.

(11) In addition to injection velocity and angle, the particle injection temperature also affects the flow substantially. Large positive values of $(t_{p0} - t_0)/(t_\infty - t_0)$ tend to increase the wall heat transfer; while near zero or negative values will decrease it, providing the viscous dissipation of particle kinetic energy is small.

(12) The effects of $c_s\mu/k$ are much more significant on the temperature distribution of the particles than of the fluid. In general, larger $c_s\mu/k$ yields higher fluid and particle temperatures and greater difference between them.

(13) For Stokes flow, particle heat convection is related to particle drag. For constant ρC_D flow, higher particle heat convection coefficient results in smaller difference between fluid and particle temperatures.

(14) Regardless of the injection velocity and angle and initial temperature, the fluid–particles relaxation effects are such that the particles decelerate vertically, accelerate or decelerate horizontally towards the upper-wall velocity, and tend to equilibrate towards the upper-wall temperature.

(15) The results of the two-phase Couette flow obtained using constant particle drag coefficient are qualitatively the same as those obtained using Stokes coefficient.

ACKNOWLEDGEMENTS

The author wishes to express his appreciation to Dr. C. W. Busch for his interest in this problem and to Mr. J. R. Taylor for the computer programming.

REFERENCES

1. G. F. Carrier, Shock waves in a dusty gas, *J. Fluid Mech.* **4**, 376–382 (1958).
2. J. R. Kliegel, Gas particle nozzle flows, *Ninth International Symposium on Combustion*, pp. 811–826. Academic Press, New York (1963).
3. F. E. Marble, Dynamics of a gas containing small solid particles, *Proceedings of the Fifth AGARD Combustion and Propulsion Colloquium*, pp. 175–215. Pergamon Press, New York (1963).
4. S. L. Soo, *Fluid Dynamics of Multiphase Systems*. Blaisdell, Massachusetts (1967).
5. J. E. Broadwell, A simple model of the non-equilibrium dissociation of a gas in Couette and boundary-layer flows, *J. Fluid Mech.* **4**, 113–139 (1958).
6. Z. O. Bleviss, Magnetogasdynamics of hypersonic Couette flow, *J. Aero/Space Sci.* **25**, 601–615 (1958).
7. R. Viskanta, Heat transfer in Couette flow of a radiating fluid with viscous dissipation, *Developments in Mechanics*, pp. 376–402. Pergamon Press, Oxford (1965).

ECOULEMENT DE COUETTE AVEC INJECTION DE PARTICULES

Résumé—On étudie l'écoulement permanent d'un fluide visqueux entre deux parois planes parallèles et infinies avec injection de particules à une paroi et extraction à l'autre. Les distributions de vitesse et de température pour le fluide et les particules sont résolues sous une forme analytique pour un coefficient de trainée de particule selon la loi de Stokes et sous forme numérique pour un coefficient constant. On suppose des valeurs arbitraires du gradient de pression axial, de la dissipation visqueuse, de l'angle et de la vitesse d'injection des particules et de la température initiale de la particule. Dans le cas d'injection verticale et en l'absence de gradient axial de pression, on trouve que l'injection de particules diminue la contrainte tangentielle alors qu'elle peut augmenter ou diminuer le transfert thermique. Les paramètres sans dimension qui caractérisent les effets de l'injection de particules sur l'écoulement de Couette avec des particules libres sont déterminés et discutés.

COUETTE-STRÖMUNG MIT TEILCHENZUFUHR

Zusammenfassung—Es wird die stationäre Strömung eines zähen Fluids untersucht zwischen zwei unendlich langen parallelen ebenen Wänden mit Zuführung von Teilchen an der einen und ihrer Abführung an der anderen Wand. Die Geschwindigkeits- und Temperaturverteilungen des Fluids und der Teilchen

werden in analytischer Form für den Stokesschen Widerstandsbeiwert der Teilchen und in numerischer Form für einen konstanten Beiwert berechnet. Die Werte des axialen Druckgradienten, viskose Dissipation, Winkel und Geschwindigkeit der zugeführten Teilchen sowie deren Anfangstemperatur sind beliebig. Im Falle senkrechter Zuführung und bei verschwindendem Druckgradienten in axialer Richtung findet man, dass die Schubspannung an der Wand infolge der Teilchenzuführung immer abnimmt, wobei der Wärmeübergang entweder ansteigt oder abnimmt. Die dimensionslosen Parameter, die die Wirkung der Teilchenzuführung auf eine teilchenfreie Couette-Strömung charakterisieren, werden analysiert und diskutiert.

ТЕЧЕНИЕ КУЭТТА СО ВДУВОМ ЧАСТИЦ

Аннотация—Проводится анализ стационарного течения вязкой жидкости между двумя бесконечными плоско-параллельными стенками при вдуве частиц через одну стенку и удалении их через другую. Получены распределения скорости и температуры жидкости и частиц в теоретической форме для коэффициента трения, описываемого законом Стокса, и в численном виде для постоянного коэффициента. Указываются произвольные значения аксиального градиента давления, вязкой диссипации, угла вдува частиц и скорости, а также начальная температура частиц. Установлено, что в случае вертикального вдува и при отсутствии аксиального градиента давления напряжение трения на стенке всегда снижается в результате вдува частиц, тогда как коэффициент теплообмена может либо уменьшаться, либо увеличиваться. Анализируется специфика полученных безразмерных параметров, характеризующих влияние вдува частиц на течение Куэтта.